RSC Advances

High performance (1-x)LiMnPO4•xLi3V2(PO4)3/C composite cathode materials prepared by sol-gel method

Journal:	*RSC Advances*
Manuscript ID	RA-ART-06-2015-011005.R1
Article Type:	Paper
Date Submitted by the Author:	19-Aug-2015
Complete List of Authors:	Li, Shanshan; Xinjiang Normal University, college of chemistry and chemical engineering; Bayingol Vocational and Technical college, Su, Zhi; Xinjiang Normal University, college of chemistry and chemical engineering Wang, Xinyu; Xinjiang Normal University, college of chemistry and chemical engineering

High performance (1-x)$LiMnPO_4 \cdot xLi_3V_2(PO_4)_3$/C composite cathode materials prepared by sol-gel method

Shanshan Li[a,b] Zhi Su[a,*] Xinyu Wang[a]

[a]***College of Chemistry and Chemical Engineering, Xinjiang Normal University, Urumqi, 830054, Xinjiang, China***

[b]***Bayingol Vocational and Technical college, Korla, 841000, Xinjiang, China.***

Abstract: A series of (1-x)$LiMnPO_4 \cdot xLi_3V_2(PO_4)_3$/C (x=0, 0.1, 0.3, 0.5, 0.7, 0.9 and 1) composite nanoparticles are synthesized as cathode materials for lithium-ion batteries by the sol-gel method, using *N*,*N*-dimethyl formamide as a dispersing agent.. The structure and morphology of the as-prepared materials are analyzed by X-ray diffraction (XRD) and transmission electron microscopy(TEM). The materials exhibit good crystallinity and a grain size of about 20-100 nm. The $0.5LiMnPO_4 \cdot 0.5Li_3V_2(PO_4)_3$/C composite delivers the best initial specific discharge capacity of 150.5mAh·g^{-1} at 0.05 C in the voltage range of 2.5-4.4 V, and it exhibits excellent reversible capacities of 150.5, 135.1, 127.0, 122.5 and 115.7 mAh·g^{-1} at charge-discharge rates of 0.05, 0.1, 0.2, 0.5, and 1 C, respectively. Finally, $0.5LiMnPO_4 \cdot 0.5Li_3V_2(PO_4)_3$/C retained 142.9 mAh·$g^{-1}$(95%) of the initial specific discharge capacity after 50 cycles, demonstrating excellent cyclability. Compared with the $LiMnPO_4$/C, its rate capability and cycle performance are both remarkably improved.

Key words: lithium manganese phosphate-lithium vanadium phosphate/carbon composite; cathode material; nanoparticles; sol-gel; electrochemical properties

***** Corresponding author. Tel.: +86- 991-4332683; fax: +86-991-4332683.

E-mail address: suzhixj@sina.com.

1. Introduction

Olivine-structured lithium transition metal phosphates ($LiMPO_4$; M = Mn, Fe, Co, and Ni) are currently receiving much attention for their potential applications as lithium ion battery cathodes given their high performance, electrochemical stability, low cost, low toxicity, and environmental friendliness [1-3]. Among them, $LiMnPO_4$ shows particular potential given its electrochemical properties; however, the inherently low ionic and electrical conductivity of this entire class of materials seriously limits Li^+ insertion and extraction and lowers charge transport rates, restricting further commercialization. Furthermore, major Jahn-Teller lattice distortions induced by Mn^{3+} result in poor cycling stability [4-8]. These disadvantages can be overcome by coating particles with a carbon layer; this decreases the interfacial resistance on the particle boundaries [9]and reduces particle size, which not only shortens the Li^+ diffusion path but the electron conduction path as well[10]. Doping with small amounts of Fe, Al, and Mg has also been reported to improve electrochemical performance [11-14].

Recently, composite materials consisting of $(1-x)LiMPO_4 \cdot xLi_3V_2(PO_4)_3/C$(M=Fe, Mn) composite materials have attracted much interest because monoclinic $Li_3V_2(PO_4)_3/C$ has excellent lithium-ion mobility owing to its more open three-dimensional framework and a high reversible capacity [15]. However, the intrinsic low electronic conductivity of LVP critically limits its high rate performance [16]. Gao et al. [17] reported the synthesis of $xLiFePO_4 \bullet yLi_3V_2(PO_4)_3/C$ composite cathode materials via a polyol process, and the $LF_{0.6}P \bullet LV_{0.4}P/C$ composite exhibited better electrochemical performance than $LiFePO_4/C$. Guo et al. [18] prepared $LiFePO_4$-$Li_3V_2(PO_4)_3/C$ composite using a modified solid-state method, and the composite exhibited excellent performance with an initial discharge capacity of 135.4 $mAh \cdot g^{-1}$ at 1C, which is higher than $LiFePO_4/C$. Bi et al.[19] synthesized $0.8LiMn_{0.8}Fe_{0.2}PO_4 \cdot 0.2Li_3V_2(PO_4)_3/C$ via high temperature solid-state reaction and $0.8LiMn_{0.8}Fe_{0.2}PO_4 \cdot 0.2Li_3V_2(PO_4)_3/C$ show better electrochemical performance. Wu et al.[20] studied the influence of $Li_3V_2(PO_4)_3$ complexing on the performance of

$LiMnPO_4$. Wang et al. [21] synthesized $xLiMnPO_4 \cdot yLi_3V_2(PO_4)_3/C$ using the solid-state method and showed that $(1-x)LiMnPO_4 \cdot xLi_3V_2(PO_4)_3/C$ composite materials had better performance than $LiMnPO_4/C$ and $Li_3V_2(PO_4)_3/C$. Qin et al.[22] reported the synthesis of $(1-x)LiMnPO_4 \cdot xLi_3V_2(PO_4)_3/C$ cathode materials, which showed good electrochemical performance, using the solid-state method with a small amount of $LiVP_2O_7$ as impurity. All of these research results reveal that compositing with $Li_3V_2(PO_4)_3$ can efficiently enhanced the electrochemical performances of $LiFePO_4$ or $LiMnPO_4$ cathode materials[17-28].

In this work, we report a series of $(1-x)LiMnPO_4 \cdot xLi_3V_2(PO_4)_3/C$ composites synthesized by the sol-gel method that employs *N*,*N*-dimethyl formamide (DMF) as a solvent. To our knowledge, there have been few reports on $(1-x)LiMnPO_4 \cdot xLi_3V_2(PO_4)_3/C$ composites synthesized via the sol-gel method. Our findings were compared with other groups' reported work on the electrochemical performance of LMP-LVP/C composite materials. It was observed that the $(1-x)LiMnPO_4 \cdot xLi_3V_2(PO_4)_3/C$ composites in this work showed no impurities compared with that reported by Qin et al. [22], and exhibited better electrochemical performance than the materials reported in the literature [21, 22]. Our findings show that the sol-gel process is a promising method to obtain the $(1-x)LiMnPO_4 \cdot xLi_3V_2(PO_4)_3/C$ composite materials with excellent electrochemical performance.

2. Experimental

2.1 Preparation of $(1-x)LiMnPO_4 \cdot xLi_3V_2(PO_4)_3/C$

All reagents used in this study were of analytical grade. First, V_2O_5 was dissolved in 10 mL H_2O_2 (30%), before 50 mL DMF was added. Second, $Mn(CH_3COO)_2 \cdot 4H_2O$ and $CH_3COOLi \cdot 2H_2O$ in stoichiometric ratio were dissolved in the solution. Meanwhile, glucose, the carbon source for the reaction, and H_3PO_4 (85% by weight) were dissolved in 30 mL DMF. The two solutions were then mixed by stirring to obtain a sol, which was dried at 40 °C overnight to yield the gel. Finally, the gel was heated at 700 °C for 12 h under an argon atmosphere before it was cooled slowly to

room temperature, yielding the (1-x)$LiMnPO_4 \cdot xLi_3V_2(PO_4)_3$/C composites.

2.2 Characterization

The microstructure of the prepared samples was characterized by X-ray diffraction (XRD, Bruker D2) with a Cu−Kα radiation source (λ=1.5408 Å) and by transmission electron microscopy (TEM, FEI Tecnai 20) with an accelerating voltage of 200 kV. The exact carbon amount has been verified by the technique using an elemental analyzer (VarioEL III, Elementar, Germany).

2.3 Electrode preparation and electrochemical tests

Electrochemical performance was assessed using coin-type half cells (LIR 2025) that were assembled in an argon glove box. The cathode materials were made from a mixture of the synthesized (1-x)$LiMnPO_4 \cdot xLi_3V_2(PO_4)_3$/C, a poly(tetrafluoroethylene) binder, and acetylene black in a 80:15:5 weight ratio. Lithium metal was used for the counter and reference electrodes, while a 1 M solution of $LiPF_6$ dissolved in a mixture of ethylene carbonate, dimethyl carbonate, and ethyl methyl carbonate in a weight ratio of 1:1:1 was used as the electrolyte. The galvanostatic method (LAND CT2001A) was used to measure the electrochemical capacity and cycle performance of the electrodes at room temperature. The charge and discharge cut-off potentials were set to 2.5 and 4.4 V versus Li^+/Li and measured at variable current densities. Cyclic voltammetry (CV, LK2500) was performed from 3.0 to 4.4 V with a scan rate of 0.1 $mV \cdot s^{-1}$. Electrochemical impedance spectroscopy (EIS, Zahner IM6ex) was completed over a frequency range of 10 kHz to 10 mHz, with a 5 mV a.c. input signal applied between the working and reference electrodes.

3. Results and discussion

As shown in the X-ray diffraction (XRD) patterns of these samples (Fig. 1), all peaks are highly ordered. The pattern of $LiMnPO_4$/C can be indexed to the standard pattern of orthorhombic LMP in ICSD #25834, and the pattern of $Li_3V_2(PO_4)_3$/C is in agreement with the standard pattern of monoclinic LVP in ICSD #96962. The peaks of both $LiMnPO_4$/C and $Li_3V_2(PO_4)_3$/C appear in the XRD patterns of the (1-x)$LiMnPO_4 \cdot xLi_3V_2(PO_4)_3$/C composites, and there are no peaks corresponding to

impurity phases. The lack of carbon diffraction peaks indicates that any carbon in the sample was amorphous [29]. The observed carbon content is about 7.0wt.% for $(1-x)LiMnPO_4 \cdot xLi_3V_2(PO_4)_3/C$.

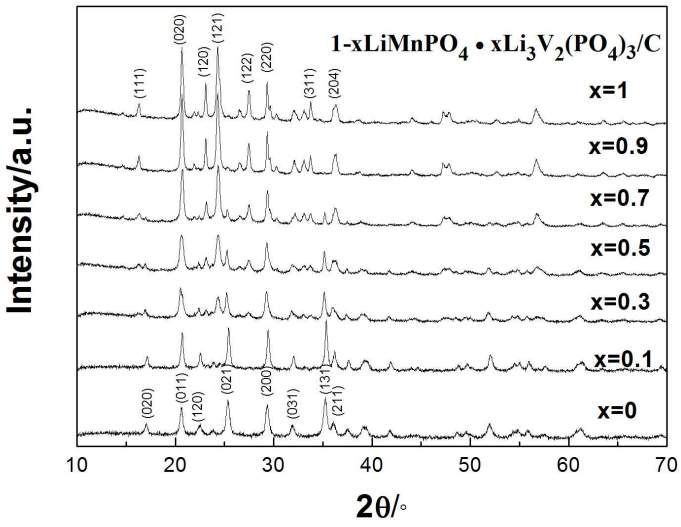

Fig. 1. XRD patterns of the $(1-x)LiMnPO_4 \cdot xLi_3V_2(PO_4)_3/C$.

TEM and HRTEM images of samples are shown in Fig. 2. Fig 2a, 2c and 2e show that the samples were observed to have similar morphologies with grain diameters of 20-100 nm. Fig 2c shows that $0.5LiMnPO_4 \cdot 0.5Li_3V_2(PO_4)_3/C$ have some reunion phenomenon. Overall, the particles are clearly dispersed throughout the carbon matrix. Sol-gel method, employing an DMF as the dispersing agent, can synthesize nanoparticles.

HRTEM images of samples are shown in Fig 2b, 2d and 2f. Fig. 2b shows that there is an evidence lattice, that can be associated with the lattice fringe of $LiMnPO_4$ (d-spacing of 0.3023 nm, lattice plane (121)). $0.5LiMnPO_4 \cdot 0.5Li_3V_2(PO_4)_3/C$(Fig. 2d) shows that there are three evidence lattices, one lattice measured to be 0.2030 nm, which is compatible with the fringe spacing values of the (122) of $LiMnPO_4$, the two other lattices of 0.3858 and 0.3360 nm are corresponding to (120) and (113) of $Li_3V_2(PO_4)_3$, respectively. Fig. 2f is found that there is one lattice fringes of $Li_3V_2(PO_4)_3$ (interplanar spacing 0.3354 nm, lattice plane (113)). The results imply that the $LiMnPO_4$ and $Li_3V_2(PO_4)_3/C$ are coexist in the composite materials. The

particles of all the samples are found to be wrapped in nanoscale carbon webs, which can provide a good electronic conduction network for the active materials[30].

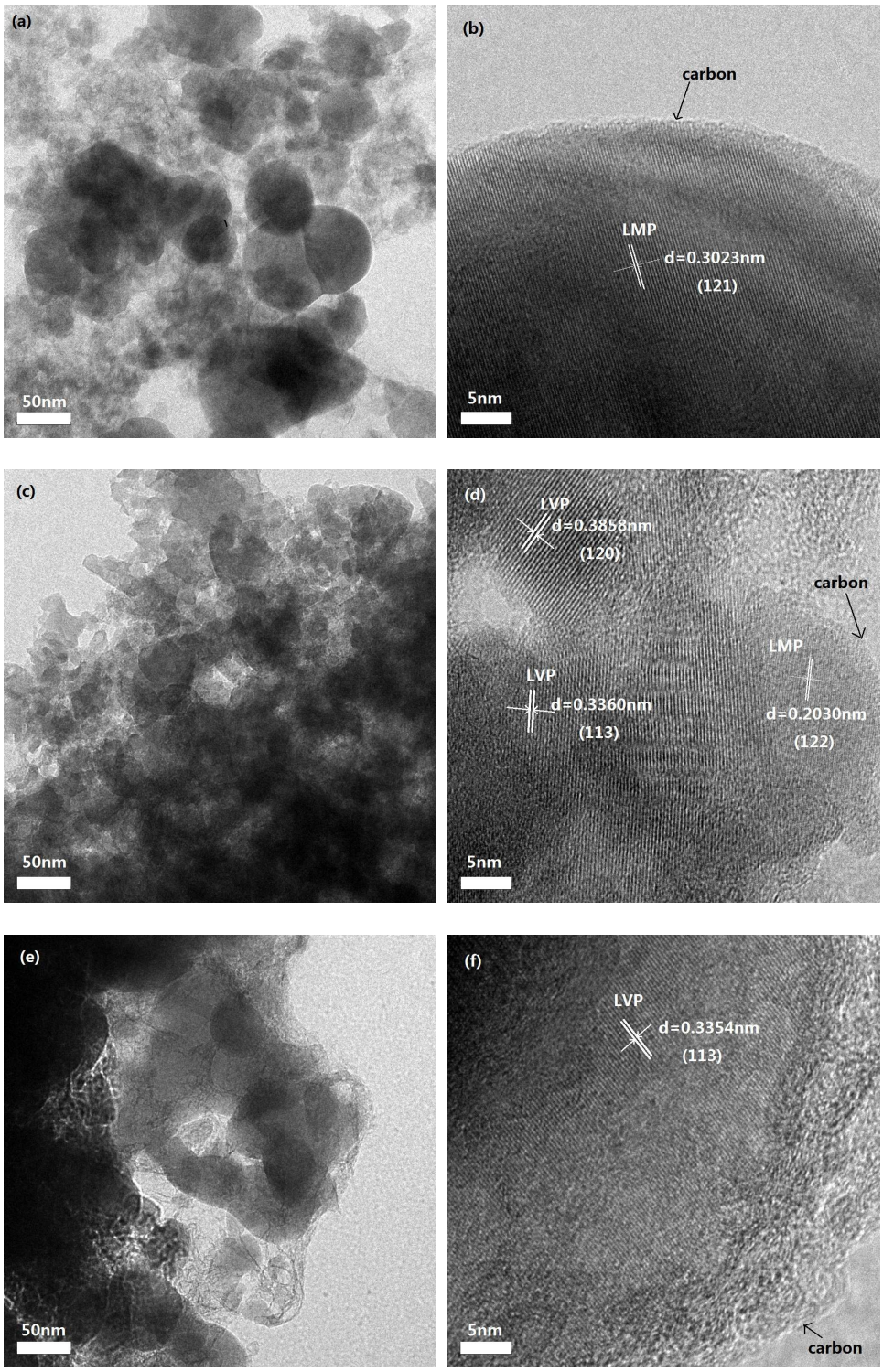

Fig. 2. TEM and HRTEM images of (a)(b) $LiMnPO_4$/C, (c)(d) $0.5LiMnPO_4 \cdot 0.5Li_3V_2(PO_4)_3$/C and (e)(f) $Li_3V_2(PO_4)_3$/C.

Fig. 3a shows the initial discharge curves of the (1-x)$LiMnPO_4 \cdot xLi_3V_2(PO_4)_3$/C samples at a charge-discharge rate of 0.05C between 2.5 and 4.4 V. Only characteristic plateaus of $LiMnPO_4$/C appears in Fig. 3a, and there are no obvious characteristic plateaus of $Li_3V_2(PO_4)_3$. When x<0.3, the materials mainly demonstrated electrochemical behavior of $LiMnPO_4$, when x> 0.7, the material mainly demonstrated electrochemical behavior of $Li_3V_2(PO_4)_3$, and when x=0.3-0.7, the plateaus of $Li_3V_2(PO_4)_3$ and $LiMnPO_4$ merge electrochemical behavior into a slowly platform between 3.0 and 4.4V, this should be attributed to synergism after two materials caused. The discharge capacity increased rapidly from x=0 for $LiMnPO_4$/C to x=0.5 for $0.5LiMnPO_4 \cdot 0.5Li_3V_2(PO_4)_3$/C, when x>0.5, the discharge capacity of the materials decreased. Fig. 3b shows the initial discharge curves of the $0.5LiMnPO_4 \cdot 0.5Li_3V_2(PO_4)_3$/C samples at different charge-discharge rates of 0.05, 0.1, 0.2, 0.5 and 1 C, discharge capacity is 150.5, 135.1, 127.0, 122.5 and 115.7 $mAh \cdot g^{-1}$,respectively. The curves demonstrate that the improved properties likely resulted from the compositing with $Li_3V_2(PO_4)_3$. Note that the $0.5LiMnPO_4 \cdot 0.5Li_3V_2(PO_4)_3$/C composite exhibited the best performance for discharge capacity.

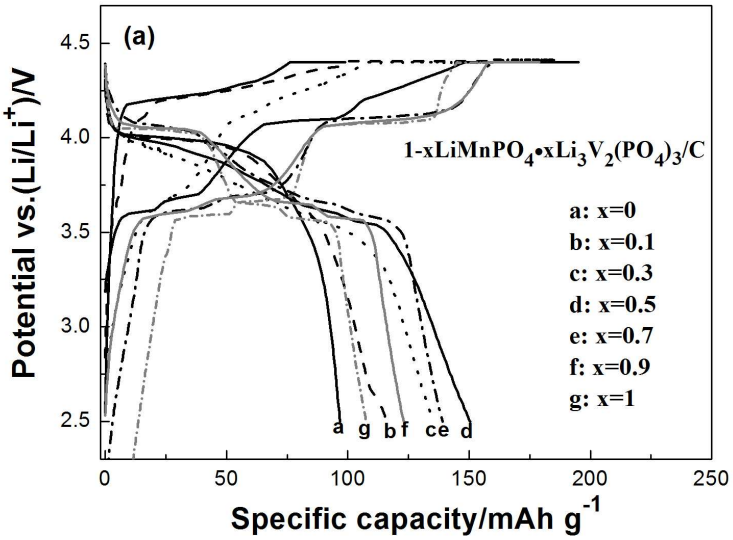

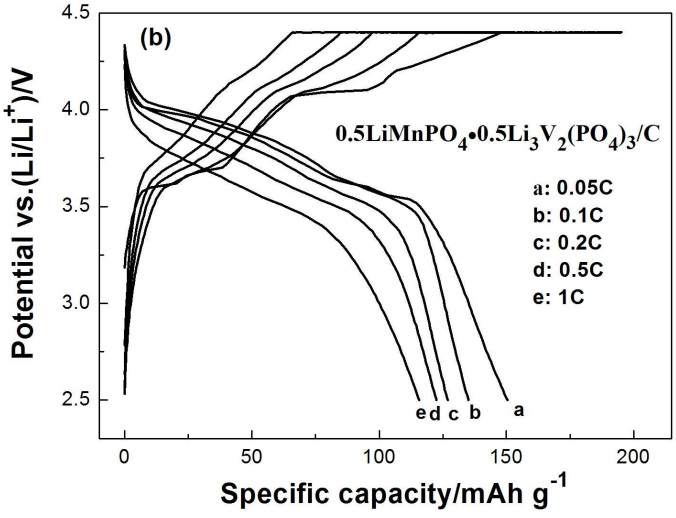

Fig. 3. Initial charge and discharge curves of (1-x)$LiMnPO_4 \cdot xLi_3V_2(PO_4)_3$/C.

Fig. 4 shows cycle life data of the (1-x)$LiMnPO_4 \cdot xLi_3V_2(PO_4)_3$/C samples at a charge-discharge rate of 0.05C. All of (1-x)$LiMnPO_4 \cdot xLi_3V_2(PO_4)_3$/C samples demonstrated excellent cycling stability, with hardly any decrease in capacity after 50 cycles. In particular, the $0.5LiMnPO_4 \cdot 0.5Li_3V_2(PO_4)_3$/C sample retained a capacity of 142.9 $mAh \cdot g^{-1}$(95%) after 50 cycles. It shows that high rate performance of samples has improved significantly after compositing with $Li_3V_2(PO_4)_3$ in Fig. 5. These improved properties likely resulted from compositing with $Li_3V_2(PO_4)_3$.

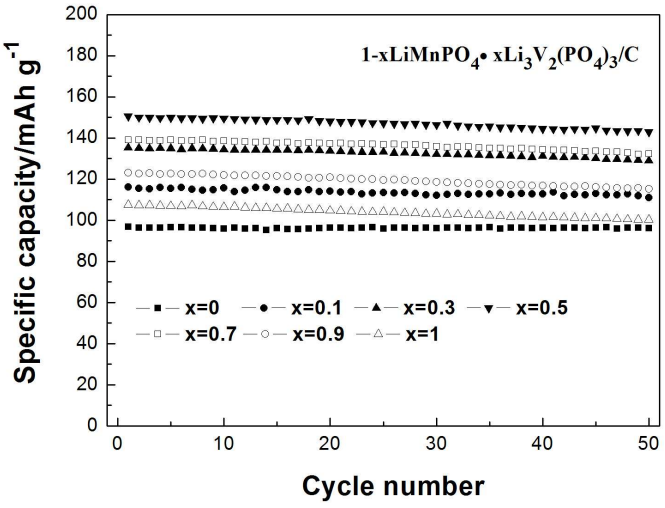

Fig. 4. Cycle life data of (1-x)$LiMnPO_4 \cdot xLi_3V_2(PO_4)_3$/C.

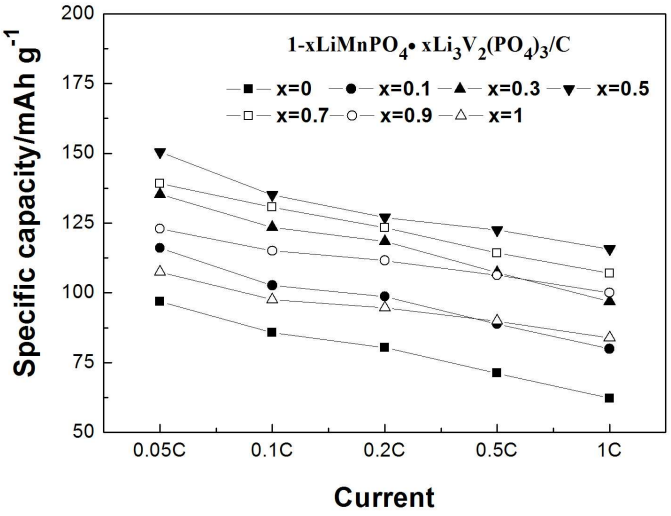

Fig. 5. Rate capacity of (1-x)$LiMnPO_4 \cdot xLi_3V_2(PO_4)_3$/C.

Fig. 6 shows the cyclic voltammetry (CV) data of both $LiMnPO_4$/C and the composite samples between 3.0 and 4.4 V at a scanning rate of 0.1mV·s^{-1}. The $LiMnPO_4$/C sample exhibited oxidation-reduction peaks at 4.37 and 3.93V, which correspond to Mn^{3+}/Mn^{2+}. Meanwhile, the composite samples exhibited three oxidation peaks and three reduction peaks corresponding to Mn^{3+}/Mn^{2+} and V^{4+}/V^{3+}. When x = 0.5, the two oxidation peaks at 4.37 V (Mn^{3+} and Mn^{2+}) and 4.11 V (V^{4+} and V^{3+}) merge to form one oxidation peak at 4.17 V. The interval between the oxidation and reduction peaks of $0.5LiMnPO_4 \cdot 0.5Li_3V_2(PO_4)_3$/C samples is smaller than that for $LiMnPO_4$/C, indicating that the reversibility of the Li insertion and extraction processes improved with the addition of $Li_3V_2(PO_4)_3$.

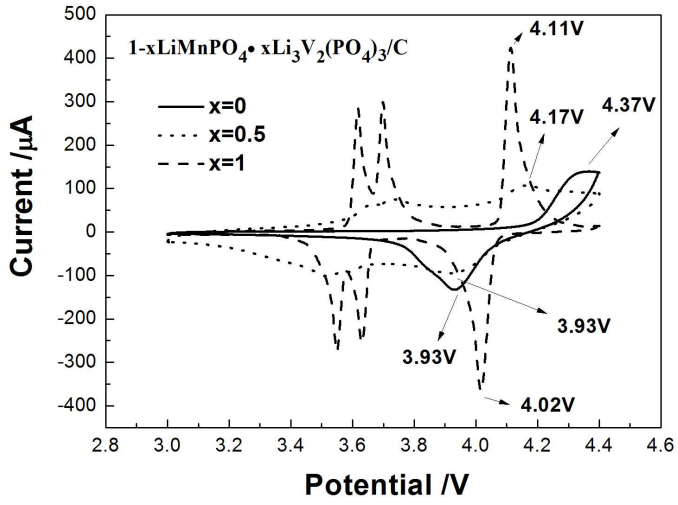

Fig. 6. Cyclic voltammogram of (1-x)$LiMnPO_4 \cdot xLi_3V_2(PO_4)_3/C$ at a sweep rate of 0.1 $mV \cdot s^{-1}$.

The electrochemical impedance spectroscopy (EIS) values of the materials were measured in a charged state after the first cycle to provide additional information on electrochemical performance. The Nyquist plots and corresponding circuits in Fig. 7 all take the shape of a semicircle in the high-frequency region and a line in the low-frequency region. The semicircle in the high-frequency region represents the charge-transfer resistance(Rct), while the line in the low-frequency region represents the Warburg impedance (Ws). The reaction was controlled by both Warburg impedance in Li^+ diffusion, which is inversely proportional to the diffusion coefficient, and the temporary, steady-state surface electrochemical reaction. Table 1 shows the calculated electrochemical parameters for all samples. Overall, the $0.5LiMnPO_4 \cdot 0.5Li_3V_2(PO_4)_3/C$ composite showed much lower charge transfer resistance and Warburg impedance than $LiMnPO_4/C$ and $Li_3V_2(PO_4)_3/C$, contributing to significantly improved Li insertion and extraction.

The plots of *Z'* against $\omega^{-1/2}$ are shown in Fig. 8. The Li-ion chemical diffusion coefficient (*D*) can be calculated from the low frequency sloping line according to the following equation[31,32]：

$$D = (0.5\ R^2\ T^2)/(\ A^2\ n^4\ F^4\ C^2\ \sigma^2) \qquad (1)$$

where D is the diffusion coefficient of lithium ion, R is the gas constant, T is the

absolute temperature, A is the surface area of the cathode, n is the number of electrons per molecule attending the electronic transfer reaction, F is the Faraday constant, C is the concentration of lithium ion, σ is the Warburg factor which is relative with Z':

$$Z' = \sigma \omega^{-1/2} \quad (2)$$

Through calculation, the diffusion coefficient is computed to be 7.54×10^{-15} $cm^2\cdot s^{-1}$ for $LiMnPO_4$, 1.84×10^{-13} $cm^2\cdot s^{-1}$ for $Li_3V_2(PO_4)_3$/C and 1.99×10^{-13} $cm^2\cdot s^{-1}$ for $0.5LiMnPO_4\cdot0.5Li_3V_2(PO_4)_3$/C. The lithium ion diffusion coefficient of $0.5LiMnPO_4\cdot0.5Li_3V_2(PO_4)_3$/C is higher than $LiMnPO_4$ and $Li_3V_2(PO_4)_3$/C. The result is in agreement with that the performance of $0.5LiMnPO_4\cdot0.5Li_3V_2(PO_4)_3$/C composite.

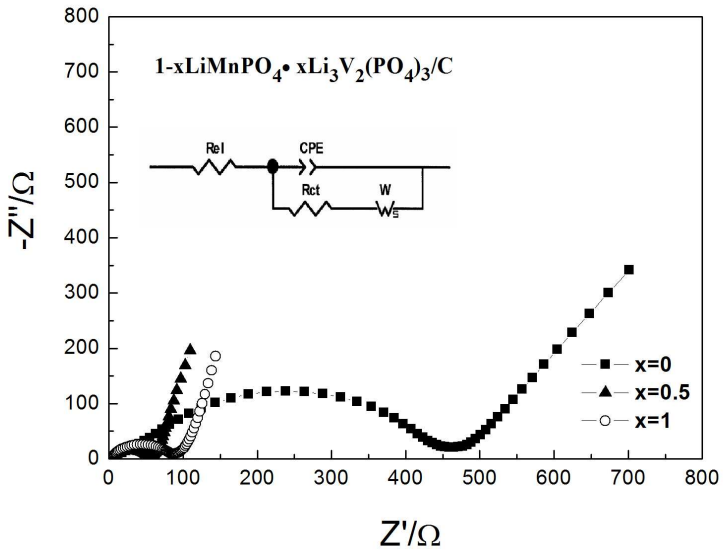

Fig. 7. Nyquist plots of $(1\text{-}x)LiMnPO_4\cdot xLi_3V_2(PO_4)_3$/C integrated into test cells.

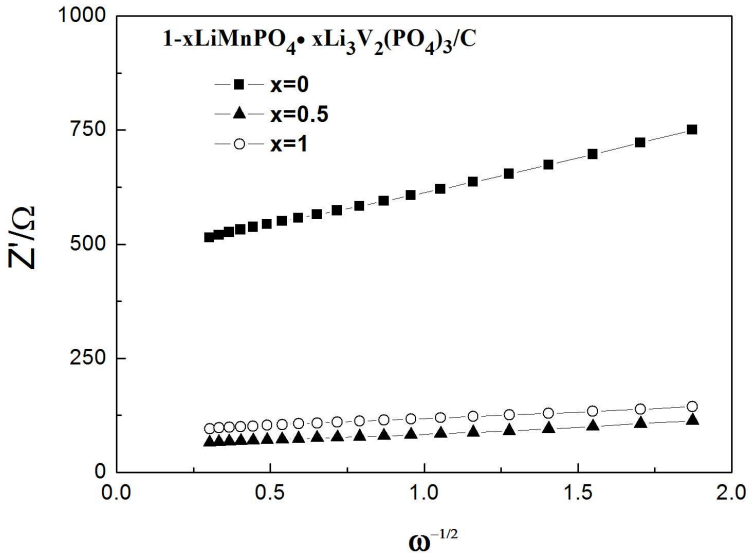

Fig. 8. The relationship between Z' and $\omega^{-1/2}$ at low frequencies

Table 1. Calculated electrochemical parameters from ac impedance spectra of the (1-x)$LiMnPO_4 \cdot xLi_3V_2(PO_4)_3/C$ samples using ZView 2.8 software[a]

Sample	Rct(Ω)	CPE($\times 10^{-4}$ F)	Ws(Ω)	D_{Li+}($cm^2 \cdot s^{-1}$)
$LiMnPO_4/C$	426.70	1.47	262.03	7.54×10^{-15}
$Li_3V_2(PO_4)_3/C$	77.22	4.05	68.35	1.84×10^{-13}
$0.5LiMnPO_4 \cdot 0.5Li_3V_2(PO_4)_3/C$	53.85	6.69	34.46	1.99×10^{-13}

[a] *R*ct represents the charge-transfer resistance, CPE represents the constant phase element, Ws represents the Warburg impedance and D_{Li+} represents Li^+ transfer coefficient.

4. Conclusion

(1-x)$LiMnPO_4 \cdot xLi_3V_2(PO_4)_3/C$ nanoparticles are successfully synthesized by the simple sol-gel method. The materials showed similar morphologies with grain diameters of about 20-100 nm, and overall excellent cycle stability. The $0.5LiMnPO_4 \cdot 0.5Li_3V_2(PO_4)_3/C$ composite delivered the best electrochemical performance, with discharge capacities of 150.5 $mAh \cdot g^{-1}$ at 0.05 C and 115.7 $mAh \cdot g^{-1}$ at 1C. The $0.5LiMnPO_4 \cdot 0.5Li_3V_2(PO_4)_3/C$ composite remains a capacity of 142.9 $mAh \cdot g^{-1}$(retention of more than 95%) after 50 cycles at 0.05C. Overall, the obtained CV and EIS data suggest that compositing with the appropriate amount of $Li_3V_2(PO_4)_3$ can efficiently improve Li insertion and extraction, as well as lithium

ion diffusion coefficient.

Acknowledgements

This study was supported by the National Natural Science Foundation of China (No.21061015), National Natural Science Foundation of China for Youth Scholars (No.21104063).

References

[1] A.K. Padhi, K.S. Nanjundaswamy, J.B. Goodenough, *J. Electrochem. Soc*.,1997, 144, 1188.

[2] J.M. Tarascon, M. Armand, *Nature*, 2001,414, 359.

[3] M.S. Whittingham, Y. Song, S. Lutta, P.Y. Zavalij, N.A. Chernova, *J. Mater. Chem.*, 2005, 15, 3362.

[4] S.Y. Chung, J.T. Bloking, Y.M. Chiang, *Nat. Mater.*, 2002, 2, 123.

[5] P. Subramanya Herle, B. Ellis, N. Coombs, L.F. Nazar, *Nat. Mater.*, 2004, 3, 147.

[6] M. Yonemura, A. Yamada, Y. Takei, N. Sonoyama, R. Kanno, *J. Electrochem. Soc.*, 2004, 151, A1352.

[7] C. Delacourt, L. Laffont, R. Bouchet, C. Wurm, *J. Electrochem. Soc.*, 2005, 152, A913.

[8] N. Meethong, H. Y. S.Huang, S. A.Speakman, *adv. Funct. Mater.*, 2007, 17, 1115.

[9] M. Maccario, L. Croguennec, A. Wattiaux, E. Suard, F. Lecras, C. Delmas, *Solid State Ionics*, 2008, 179, 2020.

[10] T. Drezen, N.-H. Kwon, P. Bowen, I. Teerlinck, M. Isono, I. Exnar, *J. Power Sources*, 2007, 174, 949.

[11] T. Muraliganth, A. Manthiram, *J. Phys. Chem. C.*, 2010, 114, 15530.

[12] G. Yang, H. Ni, H.D. Liu, P. Gao, H.M. Ji, S. Roy, J. Pinto, X.F. Jiang, *J. Power Sources*, (2011), 196, 4747.

[13] J. Kim, Y.U. Park, D.H. Seo, J. Kim, S.-W. Kim, K. Kang, *J. Electrochem. Soc.*, 2011, 158, A250.

[14] G.Y. Chen, A.K. Shukla, X.Y. Song, T.J. Richardson, *J. Mater. Chem.*, 2011, 21, 10126.

[15] J.C. Zheng, X.H. Li, Z.X. Wang, S.S. Niu, D.R. Liu, L. Wu, L.J. Li, J.H. Li, H.J. Guo, *Ionics*, 2009, 15, 753.

[16] S.C. Yin, P.S. Strobel, H. Grondey, L.F. Nazar, *Chem. Mater.*, 2004, 16, 1456.

[17] C. Gao, H. Liu, G.B. Liu, J. Zhang, W. Wang, *Materials Science and Engineering B*, 2013, 178, 272.

[18] Y. Guo , Y.D. Huang , D.Z. Jia, X.C. Wang , Neeraj Sharma, Z.P. Guo , X.C. Tang, *J. Power Sources*, 2014, 246, 912.

[19] Y.J. Bi, W.C.Yang, B.C. Yang, C.Y.Wang, D.Y. Wang, S.Q. Shi, *Ceram. Int.*, 2014, 40, 7637.

[20] L. Wu, J.J. Lu, G. Wei, P.F. Wang, H. Ding, J.W. Zheng, X.W. Li, S.K. Zhong, *Electrochim. Acta*.,2014, 146, 288.

[21] F. Wang, J. Yang, Y. N. Li , J.L. Wang, *Electrochim. Acta.*, 2013, 103, 96.

[22] L.F. Qin, Y.G. Xia , B. Qiu , H.L. Cao , Y.Z. Liu , Z.P. Liu, *J. Power Sources*, 2013, 239, 144.

[23] F. Wang, J. Yang, Y. N. Li , J.L. Wang, *Electrochim. Acta.*, 2013, 103, 96.

[24] J.Y. Xiang, J.P. Tu, L. Zhang, X.L. Wang, Y. Zhou, Y.Q. Qiao, Y. Lu, *J. Power Sources*, 2010, 195, 8331.

[25] P.P. Ma, P. Hu, Z.J. Liu, J.H. Xia, D.G. Xia, Y. Chen, Z.G. Liu, Z.C. Lu, *Electrochim. Acta.*, 2013, 106, 187.

[26] S.K. Zhong, L. Wu, J.Q. Liu, *Electrochim. Acta.*, 2012, 74, 8.

[27] L. Wu, J.J. Lu, S.K. Zhong, *J. Solid State Electrochem*., 2013, 17, 2235.

[28] J.S. Yun, S. Kim, B.W. Cho, K.Y. Lee, K.Y. Chung, W.Y. Chang, *Bull. Korean Chem. Soc.*, 2013, 34, 433.

[29] S.S. Zhang, J.L. Allen, K. Xu, *J. Power Sources*, 2005, 147, 234.

[30] S.K. Zhong, L. Wu, J.Q. Liu. *Electrochim. Acta*., 2012, 74, 8.

[31] Y. Wang, Y. Yang, Y. Yang , H. Shao, *Solid State Commun.*, 2010, 150, 81.

[32] H.J. Zhu, W. Zhai, M. Yang, X.M. Liu, Y.C. Chen, H. Yang and X.D. Shen, RSC Adv., 2014, 4, 25625